Modeling cation diffusion in compacted water-saturated Na-bentonite at low ionic strength

Ian C. Bourg[a,b,c,d,*], Garrison Sposito[a,c], and Alain C.M. Bourg[b]

[a] *Civil and Environmental Engineering, University of California, Berkeley, CA 94720-1710, USA*

[b] *Environmental HydroGeochemistry, University of Pau, BP 1155, 64013 Pau Cedex, France*

[c] *Geochemistry Department, Lawrence Berkeley National Laboratory, Berkeley, CA 94720, USA*

[d] *ANDRA, 1/7 rue Jean Monnet, 92298 Châtenay-Malabry cedex, France*

* Corresponding author. Address: Ian C. Bourg, ESPM - Sposito Lab., 137 Mulford Hall # 3114, University of California, Berkeley CA 94720, USA; email: ibourg@nature.berkeley.edu; tel: +1-510-643-3172; fax: +1-510-643-2940

Abstract

Sodium bentonites are used as barrier materials for the isolation of landfills and are under consideration for a similar use in the subsurface storage of high-level radioactive waste. The performance of these barriers is determined in large part by molecular diffusion in the bentonite pore space. We tested two current models of cation diffusion in bentonite against experimental data on the relative apparent diffusion coefficients of two representative cations, sodium and strontium. On the 'macropore/nanopore' model, solute molecules are divided into two categories, with unequal pore-scale diffusion coefficients, based on location: in macropores or in interlayer nanopores. On the 'surface diffusion' model, solute molecules are divided into categories based on chemical speciation: dissolved or adsorbed. The macropore/nanopore model agrees with all experimental data at partial montmorillonite dry densities ranging from 0.2 (a dilute bentonite gel) to 1.7 kg dm^{-3} (a highly compacted bentonite with most of its pore space located in interlayer nanopores), whereas the surface diffusion model fails at partial montmorillonite dry densities greater than about 1.2 kg dm^{-3}.

Keywords: montmorillonite, bentonite, interlayer, nanopore, diffusion, sodium, strontium.

Introduction

Sodium-bentonites (clays with high Na-montmorillonite content) are used in engineered barriers and geosynthetic liners for the isolation of landfills and polluted sites (*1*, *2*). These materials are under consideration for a similar use as barriers in the subsurface storage of high-level radioactive waste, where their low saturated hydraulic conductivity would ensure that molecular diffusion is one of the main transport processes resulting in passage through the barrier (*3*, *4*).

Efforts to predict the performance of bentonite barriers have motivated numerous experiments on solute diffusion in compacted water-saturated Na-bentonite (*5*-*13*). Measured diffusion coefficients are commonly reported as components of the apparent diffusion coefficient tensor ($\mathbf{D_a}$) defined, if $\mathbf{N}$ is the solute mass flux density and C^* is the mass of solute—both dissolved and adsorbed—per volume of porous medium, by the relation (*14*, *15*):

$$\mathbf{N} = -\mathbf{D_a} \cdot \nabla C^* \qquad (1)$$

In a recent paper, Bourg et al. (*16*) modeled the relative apparent diffusion coefficient ($D_{a,i}/D_0$, if $D_{a,i}$ is apparent diffusion coefficient in direction x_i and D_0 is the self-diffusion coefficient in bulk water) of water tracers in compacted water-saturated bentonite as a weighted sum of $D_{a,i}/D_0$ in two 'compartments' of the bentonite pore space: 'interlayer nanopores' (nanometer-scale pores located between the basal surfaces of stacked montmorillonite lamellae) and 'macropores' (all other pores), with weighting by the molar fractions of the species of interest in these two compartments ($\alpha_{macropore}$ and $\alpha_{interlayer}$, with $\alpha_{macropore} + \alpha_{interlayer} = 1$):

$$\frac{D_{a,i}}{D_0} = \alpha_{macropore}\left(\frac{D_{a,i}}{D_0}\right)_{macropore} + \alpha_{interlayer}\left(\frac{D_{a,i}}{D_0}\right)_{interlayer} \qquad (2)$$

Bourg et al. (*16*) described $D_{a,i}/D_0$ in each compartments with the relation (*17*, *18*):

$$\left(\frac{D_{a,i}}{D_0}\right)_{compartment} = \frac{\delta_{compartment}}{G_{i,compartment}} \qquad (3)$$

In eq 3, the 'geometric factor' G_i describes the influence of pore geometry (tortuosity, dead-end pores, pore-size variability) on $D_{a,i}/D_0$, and the 'constrictivity factor' δ accounts for the lower mobility of water and solutes near pore walls relative to that in bulk water. With the simplifying relations $G_{i,\text{macropore}} \approx G_{i,\text{interlayer}}$ (justified by data on water tracer diffusion in bentonite) and $\delta_{\text{macropore}} = 1$ (by definition), eqs 2 and 3 reduce to the expression (*16*):

$$\frac{D_{a,i}}{D_0} = \frac{1}{G_i}\left(\alpha_{\text{macropore}} + \alpha_{\text{interlayer}}\delta_{\text{interlayer}}\right) \qquad (4)$$

Equation 4, with a fitted mean principal geometric factor $G = 4.0 \pm 1.6$ (i.e., the average geometric factor for directions parallel and normal to compaction), is consistent with all available data on the mean principal value of the $\mathbf{D_a}$ tensor of water in Na-bentonite (*16*).

In the present study, we use eq 4 to model the diffusion of two cations, Na^+ and Sr^{2+}, having simple aqueous and surface chemistry, in compacted water-saturated Na-bentonite hydrated by low-ionic-strength solutions at 298 K. Unfortunately, data on Na^+ and Sr^{2+} diffusion in compacted Na-bentonite are available only for the $D_{a,//}$ component (in the direction parallel to bentonite compaction, $x_{//}$) of the $\mathbf{D_a}$ tensor. The unknown $G_{//}$-value, considered to vary with bentonite dry bulk density, is routinely estimated by fitting a diffusion model to experimental data on the diffusion of water tracers in bentonite in the $x_{//}$ direction (*5*, *14*, *19-22*). With this method, eq 4 yields a testable model of the ratio of relative apparent diffusion coefficients of cations and water tracers:

$$\frac{\left(D_{a,//}/D_0\right)_{\text{cation}}}{\left(D_{a,//}/D_0\right)_{\text{water}}} = \frac{\alpha_{\text{macropore,cation}} + \alpha_{\text{interlayer,cation}}\delta_{\text{interlayer,cation}}}{\alpha_{\text{macropore,water}} + \alpha_{\text{interlayer,water}}\delta_{\text{interlayer,water}}} \qquad (5)$$

With the approximations $\alpha_{\text{interlayer,water}} \approx f_{\text{interlayer}}$ [if $f_{\text{interlayer}}$ is the volume fraction of bentonite pore space located in nanopores (*16*)] and $\alpha_{\text{interlayer,cation}} \approx 1$ (in bentonite hydrated by low-ionic-

strength solutions), we obtain the form of the macropore/nanopore model used in the present paper [where $f_{\text{interlayer}}$ and $\delta_{\text{interlayer,water}}$ are known (*16*)]:

$$\frac{\left(D_{a,//}/D_0\right)_{\text{cation}}}{\left(D_{a,//}/D_0\right)_{\text{water}}} = \frac{\delta_{\text{interlayer,cation}}}{\left(1-f_{\text{interlayer}}\right)+f_{\text{interlayer}}\delta_{\text{interlayer,water}}} \qquad (6)$$

The main alternative to eq 4 is the 'surface diffusion model' (*5*, *19*, *23*, *24*):

$$\frac{D_{a,i}}{D_0} = \frac{1}{G_i}\frac{\varepsilon+\rho_b K_d\left(\frac{D_s}{D_0}\right)}{\varepsilon+\rho_b K_d} \qquad (7)$$

where ε and ρ_b are the porosity and dry bulk density, K_d is the distribution coefficient ($K_d \equiv q/C$, if q and C are the amounts of adsorbed cation per mass of solid and of dissolved cation per volume of pore space, at equilibrium), and D_s is a 'surface diffusion coefficient'. In practice, G_i is determined by fitting eq 7 to experimental data on water tracer diffusion (*5*, *19*), i.e., the surface diffusion model is effectively used as a model of the ratio of relative apparent diffusion coefficients of cations and water tracers:

$$\frac{\left(D_{a,//}/D_0\right)_{\text{cation}}}{\left(D_{a,//}/D_0\right)_{\text{water}}} = \frac{\varepsilon+\rho_b K_d\left(\frac{D_s}{D_0}\right)_{\text{cation}}}{\varepsilon+\rho_b K_d} \qquad (8)$$

In bentonite hydrated by low ionic-strength solutions, most cations are adsorbed ($\rho_b K_d >> \varepsilon$), and eq 8 reduces to the expression:

$$\frac{\left(D_{a,//}/D_0\right)_{\text{cation}}}{\left(D_{a,//}/D_0\right)_{\text{water}}} = \left(\frac{D_s}{D_0}\right)_{\text{cation}} \qquad (9)$$

In the present article, the macropore/nanopore and surface diffusion models (eqs 6 and 9) are compared with available experimental data on $(D_{a,//}/D_0)_{\text{cation}}/(D_{a,//}/D_0)_{\text{water}}$ in compacted bentonite hydrated by low ionic-strength solutions. Model predictions are obtained, with no fitted parameters, from independent estimates of $\delta_{\text{interlayer,cation}}$ and $(D_s/D_0)_{\text{cation}}$.

Experimental data on $D_{a,i}/D_0$ of water tracers, Na^+ and Sr^{2+}.

Experimental data on the relative apparent diffusion coefficients of trace isotopes of water, sodium or strontium in one-dimensionally compacted, water-saturated Na-bentonite are plotted in Figure 1 against partial montmorillonite dry density ($\rho_{b,mont}$), the mass of montmorillonite per combined volume of montmorillonite and pore space. Diffusion was measured using isotopic tracers (HDO, HTO, $^{22}Na^+$ and $^{85}Sr^{2+}$) in directions parallel ($x_{//}$) or normal ($x_{\perp}$) to compaction. Experimental results were obtained at constant and uniform macroscopic-scale properties (temperature, porosity, dry bulk density, montmorillonite content of the bentonite) with bentonites almost devoid of readily-soluble non-montmorillonitic impurities [Kunipia-F bentonite, used by Sato and coworkers (*8*, *10*, *14*), contains 99 ± 1 % montmorillonite by mass; Kozaki and coworkers used purified Kunipia-F bentonite (*11*, *25-29*) or mixtures of purified Kunipia-F and silica sand (*6*, *7*)] and saturated by pure water or low ionic-strength solutions. Partial montmorillonite dry densities, D_a-values (slightly extrapolated to 298 K) and confidence intervals ($\pm 2\sigma$) were calculated as in Bourg (*28*) and Bourg et al. (*16*).

Independent estimates of $\delta_{interlayer,cation}$.

$\delta_{interlayer,Na}$. Van Schaik et al. (*31*) measured the apparent diffusion coefficients of water, sodium and chloride isotopic tracers in water-saturated Na-montmorillonite at $\rho_{b,mont} \approx 1.1$ kg dm^{-3}, estimated the geometric factor by comparing water diffusion in their experiments and in films of oriented montmorillonite lamellae of same clay/water ratio (*32*), and deduced $\delta_{interlayer,Na} = 0.32 \pm 0.06$, on average, for Na-montmorillonite hydrated by 0.0038 to 0.15 mol dm^{-3} NaCl solutions. Estimates of the constrictivity factor of interlayer sodium ions obtained by other methods are

consistent with the results of van Schaik et al. (*31*): Mott (*33*) reported apparent diffusion coefficients of sodium in films of oriented lamellae of Na-montmorillonite at low relative humidity that suggest $\delta_{interlayer,Na} \approx 0.08\text{-}0.43$ in the two- and three-layer hydrates (*28*); molecular dynamics (MD) simulations of montmorillonite interlayer nanopores by Chang et al. (*34*) and Marry and Turq (*35*) yield $\delta_{interlayer,Na} = 0.41 \pm 0.23$ (with a confidence interval of $\pm\sigma$, vs. $\pm 2\sigma$ elsewhere in this paper) in the two- and three-layer hydrates of Na-montmorillonite having structural charge located mainly in the octahedral sheet (*28*).

$\delta_{interlayer,Sr}$. Calvet (*36*) measured the apparent diffusion coefficients of sodium and calcium ions in unsaturated Na/Ca-montmorillonite with varying amounts of exchangeable calcium and sodium at water contents corresponding to the one- and two-layer hydrates. His results yield $\delta_{interlayer,Ca}/\delta_{interlayer,Na} = 0.25 \pm 0.05$ in the one- and two-layer hydrates of Na-montmorillonite (*28*). If $\delta_{interlayer,Ca} \approx \delta_{interlayer,Sr}$, as expected from the nearly-identical diffusion coefficients of strontium and calcium in bulk water (*17*) and the similar cation-exchange constants for the two ions on montmorillonite (*37*), the constrictivity factor of sodium determined in the previous paragraph yields $\delta_{interlayer,Sr} = 0.080 \pm 0.022$. The result $\delta_{interlayer,Na} > \delta_{interlayer,Sr}$ is not unexpected: on a time-scale of ~100 ps, MD simulations of Na-montmorillonite two-layer hydrates reveal a diffusive motion of interlayer sodium with extensive exchange of water molecules into and out of its first solvation shell (*34*), whereas electron spin resonance spectra of Sr-montmorillonite two-layer hydrates show little motion of the stable interlayer strontium solvation complex (*38*).

Results and discussion

We solved eqs 6 and 9 with $\delta_{interlayer,water} = 0.30 \pm 0.05$ (*16*), $\delta_{interlayer,Na} = 0.32 \pm 0.06$, $\delta_{interlayer,Sr} = 0.080 \pm 0.022$, and $(D_s/D_0)_{cation} \approx \delta_{interlayer,cation}$ (because most interlayer nanopore cations are

147 adsorbed and most adsorbed cations are located in interlayer nanopores). We calculated $f_{\text{interlayer}}$
148 as in Bourg et al. (*16*), using the x-ray diffraction data of Kozaki et al. (*26*). Model predictions
149 obtained with eqs 6 and 9 are compared with experimental data in Figure 2. The
150 macropore/nanopore model, although strictly valid only in the range $\rho_{b,mont}$ = 0.98 to 1.72 kg dm^{-3}
151 [where x-ray diffraction data reveal the existence of two- or three-layer hydrates (*26*)], agrees
152 with all available experimental data for $\rho_{b,mont} \geq 0.2$ kg dm^{-3}. The surface diffusion model is
153 successful only at low values of $\rho_{b,mont}$. At $\rho_{b,mont} > 1.3$ kg dm^{-3}, if $G_{//}$ is determined from water
154 tracer diffusion data, the surface diffusion model underestimates cation D_a-values by a factor of
155 about two.

156 The surface diffusion and macropore/nanopore models differ mainly in the categories used
157 in each model to distinguish molecules whose pore-scale self-diffusion coefficient is affected by
158 the pore walls from those which are not affected. In the surface diffusion model, the categories
159 are based on the thermodynamic concept of adsorption: a Gibbs surface excess of the species of
160 interest expressed relative to water as a non-adsorbing reference (*39*). Thus all bentonite pore
161 water is free water by definition, and its pore diffusion coefficient, according to the surface
162 diffusion model, is equal to the diffusion coefficient of a tracer in bulk water even in the
163 narrowest nanopores. By contrast, in the macropore/nanopore model, the categories are based on
164 the physical location of the molecules (in macropores or in interlayer nanopores), and all
165 interlayer species, even water tracers, are assigned properties differing from those of the same
166 species in macropores or bulk water. As a result, the surface diffusion model predicts that
167 $(D_a/D_0)_{cation}/(D_a/D_0)_{water}$ is independent of $\rho_{b,mont}$ in bentonite equilibrated with pure water
168 (because most cations are adsorbed and all water is free, independently of $\rho_{b,mont}$), whereas the

169 macropore/nanopore model predicts that $(D_a/D_0)_{cation}/(D_a/D_0)_{water}$ increases with $\rho_{b,mont}$ (because
170 the fraction of pore water located in interlayer nanopores increases with $\rho_{b,mont}$).

171 The inclusion of a distinct interlayer nanopore compartment into models of chemical,
172 hydraulic, thermal and mechanical processes is an emerging concept in studies of clay barriers
173 (*2*, *16*, *40-44*). As shown here and in Bourg et al. (*16*), if the relevant properties of interlayer
174 species can be determined independently, the use of a distinct interlayer nanopore compartment
175 can improve model performance while *decreasing* the number of fitted parameters.

176 Several choices made in constructing the macropore/nanopore model deserve further
177 attention. Firstly, the nanopore compartment of eq 4 could have been subdivided into two- and
178 three-layer hydrate 'sub-compartments' (designated with subscripts "2-layer" and "3-layer") to
179 yield the generalized relation:

180 $$\frac{D_{a,i}}{D_0} = \frac{1}{G_i}\left(\alpha_{\text{macropore}} + \alpha_{\text{2-layer}}\delta_{\text{2-layer}} + \alpha_{\text{3-layer}}\delta_{\text{3-layer}}\right) \qquad (10)$$

181 The fact that eq 4 is sufficient to describe all experimental data in Figure 2 and in Bourg et al.
182 (*16*) indicates that $\delta_{2\text{-layer}} \sim \delta_{3\text{-layer}}$ for water tracers, sodium and strontium diffusing in Na-
183 bentonite at 298 K. The distinction between two- and three-layer hydrate sub-compartments may
184 be useful, however, for other solutes or at temperatures other than 298 K (*28*).

185 Secondly, all montmorillonite basal surfaces were treated as interlayer nanopore walls in
186 the calculation of $f_{\text{interlayer}}$ (*16*). This simplification is strictly valid only if montmorillonite stacks
187 are sufficiently thick that their external basal surfaces can be neglected, or if a layer of pore
188 water on external basal surfaces with a thickness of half of the average interlayer distance
189 behaves as interlayer water. In a manner similar to that proposed in the previous paragraph, the
190 interlayer nanopore compartment of eq 4 could be subdivided into 'internal basal surface' and
191 'external basal surface' sub-compartments. The distinction between internal and external basal

surfaces may be necessary to describe the activation energy of diffusion of cations in water-saturated bentonite near $\rho_{b,mont}$ = 1.0 kg dm^{-3} (*11*). At present, few data allow a comparison of solute self-diffusion coefficients on internal and external basal surfaces. Scarce MD simulation results suggest that sodium ions have similar self-diffusion coefficients on internal and external basal surfaces of smectite clay minerals (*45*).

Thirdly, the relation $\alpha_{macropore} + \alpha_{interlayer} = 1$ used in the macropore/nanopore model implies that all solute molecules are located either in macropores or in interlayer nanopores. In reality, a fraction of cations in water-saturated bentonite may be bound to oxide-type surface sites on montmorillonite edges or on non-montmorillonitic solids (*43*). If adsorption on such sites results in solute immobilization on time-scales much longer than that of molecular-scale diffusive motions, eq 4 should be solved under the constraint $\alpha_{macropore} + \alpha_{interlayer} + \alpha_{oxide} = 1$, where α_{oxide} is the mole fraction of the species of interest adsorbed on oxide-type sites. Experimental data on the pH-dependence of $^{22}Na^{+}$ adsorption on Na-montmorillonite and Na-bentonite in 0.01-0.1 mol dm^{-3} sodium electrolytes (*5*, *46*) indicate that $\alpha_{oxide}/\alpha_{interlayer} < 0.1$ for sodium at all pH values. For strontium, adsorption on oxide-type sites of Na-montmorillonite is significant at alkaline pH values and ionic strengths greater than about 0.1 mol dm^{-3} (*5*, *47*). Wang and Liu (*9*) reported an approximately 40 % decrease in strontium D_a-values in Na-bentonite (at $\rho_{b,mont}$ = 0.8 kg dm^{-3} and ionic strength I = 0.1 mol dm^{-3} $NaClO_4$) as pH increased from 6.5 to 9, a result consistent with the hypothesis of a temporary immobilization of about 40 % of the strontium ions by adsorption on oxide-type edge surface sites at pH 9. Because oxide-type sites were neglected in eq 4 and in our analysis of the data of Calvet (*36*), their possible influence on strontium diffusion, in the present study, is effectively included in the parameter $\delta_{interlayer,Sr}$.

214 Four decades ago, van Schaik et al. (*31*) proposed that $\delta_{interlayer,cation}$ is equal to the product
215 of two terms: (1) the "relative fluidities of solution surrounding the adsorbed diffuse layer
216 cations and free electrolyte cations" and (2) the mole fraction of cations located in the diffuse
217 layer (cations adsorbed in the 'Stern layer', i.e., inner- and outer-sphere surface complexes, were
218 presumed immobile). Li and Gregory (*17*) and Kato et al. (*48*) stressed the importance of the first
219 term ["the ratio of viscosity of the bulk solution to the average viscosity of interstitial solution"
220 (*17*)], while the second term was included in several variants of the surface diffusion model (*5*,
221 *21*, *22*, *49*). Other factors may affect to $\delta_{interlayer}$, such as water and solute exchange rates across
222 the macropore/nanopore boundary (*28*, *50*). Further investigation of the processes that control
223 $\delta_{interlayer}$ may allow a generalization of the macropore/nanopore diffusion model to include other
224 solutes, temperatures or types of clay minerals than those investigated in the present study.
225
226 **Acknowledgements**
227 The first author (ICB) is grateful for a predoctoral fellowship from the French Agency for
228 Radioactive Waste Management (ANDRA, Agence Nationale pour la Gestion des Déchets
229 Radioactifs, Châtenay-Malabry, France). The data analysis reported in this paper also was
230 supported in part by the Director, Office of Energy Research, Office of Basic Energy Sciences,
231 of the US Department of Energy under Contract No. DE-AC03-76F00098. The interpretation of
232 experimental diffusion data benefited greatly from discussions between the first author and
233 Professor T. Kozaki, Hokkaido University (Japan).

References

(1) LaGrega, M.D.; Buckingham, P.L.; Evans, J.C. *Hazardous Waste Management*, 2nd Ed.; McGraw-Hill: Boston, 2001.

(2) Jo, H.Y.; Benson, C.H.; Edil, T.B. Rate-limited cation exchange in thin bentonitic barrier layers. *Can. Geotech. J.* **2006**, *43*, 370-391.

(3) SKB. *Interim process report for the safety assessment SR-Can*; SKB Report R-04-33, SKB: Stockholm, 2004.

(4) Montes-H, G.; Marty, N.; Fritz, B.; Clement, A.; Michau, N. Modelling of long-term diffusion-reaction in a bentonite barrier for radioactive waste confinement. *Appl. Clay Sci.* **2005**, *30*, 181-198.

(5) Molera, M.; Eriksen, T. Diffusion of $^{22}Na^{+}$, $^{85}Sr^{2+}$, $^{134}Cs^{+}$ and $^{57}Co^{2+}$ in bentonite clay compacted to different densities: experiments in modeling. *Radiochim. Acta* **2002**, *90*, 753-760.

(6) Liu, J.; Yamada, H.; Kozaki, T.; Sato, S.; Ohashi, H. Effect of silica sand on activation energy for diffusion of sodium ions in montmorillonite and silica sand mixture. *J. Contam. Hydrol.* **2003**, *61*, 85-93.

(7) Liu, J.; Kozaki, T.; Horiuchi, Y.; Sato, S. Microstructure of montmorillonite/silica sand mixture and its effects on the diffusion of strontium ions. *Appl. Clay Sci.* **2003**, *23*, 89-95.

(8) Sato, H.; Suzuki, S. Fundamental study on the effect of an orientation of clay particles on diffusion pathway in compacted bentonite. *Appl. Clay Sci.* **2003**, *23*, 51-60.

(9) Wang, X.; Liu, X. Effect of pH and concentration on the diffusion of radiostrontium in compacted bentonite—a capillary experimental study. *Appl. Radiat. Isot.* **2004**, *61*, 1413-1418.

(10) Suzuki, S.; Sato, H.; Ishidera, T.; Fujii, N. Study on anisotropy of effective diffusion coefficient and activation energy for deuterated water in compacted sodium bentonite. *J. Contam. Hydrol.* **2004**, *68*, 23-37.

(11) Kozaki, T.; Fujishima, A.; Saito, N.; Sato, S.; Ohashi, H. Effects of dry density and exchangeable cations on the diffusion process of sodium ions in compacted montmorillonite. *Eng. Geol.* **2005** *81*, 246-254.

(12) Sato, H. Effects of the orientation of smectite particles and ionic strength on diffusion and activation enthalpies of I^- and Cs^+ ions in compacted smectite. *Appl. Clay Sci.* **2005**, *29*, 267-281.

(13) Glaus, M.A.; Baeyens, B.; Bradbury, M.H.; Jakob, A.; Van Loon, L.R.; Yaroshchuk, A. Diffusion of ^{22}Na and ^{85}Sr in montmorillonite: Evidence of interlayer diffusion being the dominant pathway at high compaction. *Environ. Sci. Technol.* **2007**, *41*, 478-485.

(14) Sato, H.; Ashida, T.; Kohara, Y.; Yui, M.; Sasaki, N. Effect of dry density on diffusion of some radionuclides in compacted sodium bentonite. *J. Nucl. Sci. Technol.* **1992**, *29*, 873-882.

(15) Muurinen, A. *Diffusion of anions and cations in compacted sodium bentonite*; Ph.D. Thesis, VTT Publications 168, Technical Research Centre of Finland: Espoo, 1994.

(16) Bourg, I.C.; Sposito, G.; Bourg, A.C.M. Tracer diffusion in compacted water-saturated bentonite. *Clays Clay Miner*. **2006**, *54*, 363-374.

(17) Li, Y.-H.; Gregory, S. Diffusion of ions in sea water and in deep-sea sediments. *Geochim. Cosmochim. Acta* **1974**, *38*, 703-714.

(18) Boving, T.B.; Grathwohl, P. Tracer diffusion coefficients in sedimentary rocks: correlation to porosity and hydraulic conductivity. *J. Contam. Hydrol*. **2001**, *53*, 85-100.

(19) Jensen, D.J., Radke, C.J. Caesium and strontium diffusion through sodium montmorillonite at elevated temperature, *J. Soil Sci.* **1988**, *39*, 53-64.

(20) Choi, J.-W., Oscarson, D.W. Diffusive transport through compacted Na- and Ca-bentonite, *J. Contam. Hydrol.* **1996**, *22*, 189-202.

(21) Lehikoinen, J.; Muurinen, A.; Valkainen, M. A consistent model for anion exclusion and surface diffusion. In *Scientific Basis for Nuclear Waste Management XXII*; Wronkiewicz, D., Lee, J., Eds.; Materials Research Society: Pittsburgh, 1999; pp 663-670.

(22) Ochs, M.; Lothenbach, B.; Wanner, H.; Sato, H.; Yui, M. An integrated sorption-diffusion model for the calculation of consistent distribution and diffusion coefficients in compacted bentonite. *J. Contam. Hydrol*. **2001**, *47*, 283-296.

(23) Nye, P.H. Diffusion of ions and uncharged solutes in soils and soil clays. *Adv. Agron*. **1979**, *31*, 225-272.

(24) Lehikoinen, J.; Carlsson, T.; Muurinen, A.; Olin, M.; Salonen, P. Evaluation of factors affecting diffusion in compacted bentonite. In *Scientific Basis for Nuclear Waste Management XIX*; Murphy, W.M., Knecht, K.A., Eds.; Materials Research Society: Pittsburgh, 1996; pp 675-682.

(25) Kozaki, T.; Sato, H.; Fujishima, A.; Saito, N.; Sato, S.; Ohashi, H. Effect of dry density on the activation energy for diffusion of strontium in compacted sodium montmorillonite. In *Scientific Basis for Nuclear Waste Management XX*; Gray, W.J., Triay, I.R., Eds.; Materials Research Society: Pittsburgh, 1997; pp 893-900.

(26) Kozaki, T.; Fujishima, A.; Sato, S.; Ohashi, H. Self-diffusion of sodium ions in compacted sodium montmorillonite. *Nucl. Technol*. **1998**, *121*, 63-69.

(27) Kozaki, T.; Sato, Y.; Nakajima, M.; Kato, H.; Sato, S.; Ohashi, H. Effect of particle size on the diffusion behavior of some radionuclides in compacted bentonite. *J. Nucl. Mater.* **1999**, *270*, 265-272.

(28) Bourg, I.C. *Diffusion of water and inorganic ions in saturated compacted bentonite*; Ph.D. Thesis, University of California: Berkeley, 2004.

(29) Mills, R. Self-diffusion in normal and heavy water in the range 1-45°. *J. Phys. Chem.* **1973**, *77*, 685-688.

(30) Wang, J.H.; Miller, S. Tracer-diffusion in liquids. II. The self-diffusion of sodium ion in aqueous sodium chloride solutions. *J. Am. Chem. Soc.* **1952**, *74*, 1611-1612.

(31) van Schaik, J.C.; Kemper, W.D.; Olsen, S.R. Contribution of adsorbed cations to diffusion in clay-water systems. *Soil Sci. Soc. Am. Proc*. **1966**, *30*, 17-22.

(32) Kemper, W.D.; Maasland, D.E.L.; Porter L. Mobility of water adjacent to mineral surfaces. *Soil Sci. Soc. Am. Proc*. **1964**, *28*, 164-167.

(33) Mott, C.J.B. Ph.D. Thesis, Oxford University: Oxford, 1967. Cited in Nye (*23*).

(34) Chang, F.-R.C.; Skipper, N.T.; Sposito, G. Computer simulation of interlayer molecular structure in sodium montmorillonite interlayer. *Langmuir* **1995**, *11*, 2734-2741.

(35) Marry, V.; Turq, P. Microscopic simulations of interlayer structure and dynamics in bihydrated heteroionic montmorillonites. *J. Phys. Chem. B* **2003**, *107*, 1832-1839.

(36) Calvet, R. Hydratation de la montmorillonite et diffusion des cations compensateurs. *Ann. Agron.* **1973**, *24*, 77-217.

(37) Fletcher, P.; Sposito, G. The chemical modelling of clay/electrolyte interactions for montmorillonite. *Clay Miner*. **1989**, *24*, 375-391.

(38) McBride, M.B.; Pinnavaia, T.J.; Mortland, M.M. Electron spin resonance studies of cation orientation in restricted water layers on phyllosilicate (smectite) surfaces. *J. Phys. Chem.* **1975**, *79*, 2430-2435.

(39) Sposito, G. *The Surface Chemistry of Natural Particles*; Oxford University Press: Oxford, 2004.

(40) Hueckel, T.; Loret, B.; Gajo, A. Expansive clays as two-phase, deformable reactive continua: Concepts and modeling options. In *Chemo-Mechanical Coupling in Clays*; Di Maio, C., Hueckel, T., Loret, B., Eds.; Balkema Publ.: Lisse, 2002; pp 105-120.

(41) Bradbury, M.; Baeyens, B. Porewater chemistry in compacted re-saturated MX-80 bentonite. *J. Contam. Hydrol*. **2003**, *61*, 329-338.

(42) Ichikawa, Y.; Kawamura, K.; Fujii, N.; Kitayama, K. Microstructure and micro/macro-diffusion behavior of tritium in bentonite. *Appl. Clay Sci*. **2004**, *26*, 75-90.

(43) Wersin, P.; Curti, E.; Appelo, C.A.J. Modelling bentonite-water interactions at high solid/liquid ratios: swelling and diffuse double layer effects. *Appl. Clay Sci*. **2004**, *26*, 249-257.

(44) Xie, M.; Bauer, S.; Kolditz, O.; Nowak, T.; Shao, H. Numerical simulation of reactive processes in an experiment with partially saturated bentonite. *J. Contam. Hydrol*. **2006**, *83*, 122-147.

(45) Leote de Carvalho, R.J.F.; Skipper, N.T. Atomistic computer simulation of the clay-fluid interface in colloidal laponite. *J. Chem. Phys*. **2001**, *114*, 3727-3733.

(46) Zachara, J.M.; McKinley, J.P. Influence of hydrolysis on the sorption of metal cations by smectites: Importance of edge coordination reactions. *Aquat. Sci*. **1993**, *55*, 250-261.

(47) Chen, C.C.; Hayes, K.F. X-ray absorption spectroscopy investigation of aqueous Co(II) and Sr(II) sorption at clay-water interfaces. *Geochim. Cosmochim. Acta* **1999**, *63*, 3205-3216.

(48) Kato, H.; Muroi, M.; Yamada, N.; Ishida, H.; Sato, H. Estimation of effective diffusivity in compacted bentonite. In *Scientific Basis for Nuclear Waste Management XVIII*; Murakami, T., Ewing, R.C., Eds.; Materials Research Society: Pittsburgh, 1995; pp 277-284.

(49) Leroy, P.; Revil, A.; Coelho, D. Diffusion of ionic species in bentonite. *J. Colloid Interface Sci.* **2006**, *296*, 248-255.

(50) Rotenberg, B.; Marry, V.; Vuilleumier, R.; Malikova, N.; Simon, C.; Turq, P. Water and ions in clays: Unraveling the interlayer/micropore exchange using molecular dynamics. *Geochim. Cosmochim. Acta*, submitted.

List of Figures

Figure 1. Relative apparent diffusion coefficients of water, sodium and strontium in one-dimensionally compacted, water-saturated Na-bentonite at 298 K, plotted as a function of partial montmorillonite dry density. Data were measured in direction parallel ($D_{a,//}/D_0$, filled symbols) or normal to bentonite compaction ($D_{a,\perp}/D_0$, open symbols). Relative apparent diffusion coefficients were calculated with D_0 = 2.27 and 2.24 × 10^{-9} m^2 s^{-1} for HDO and HTO (*29*), 1.33 × 10^{-9} m^2 s^{-1} for Na^+ (*30*) and 0.79 × 10^{-9} m^2 s^{-1} for Sr^{2+} (*17*).

Figure 2. Ratio of the relative apparent diffusion coefficients of cations and water tracers in water-saturated bentonite at 298 K (calculated from data in Figure 1), plotted as a function of partial montmorillonite dry density. Predictions obtained with the surface diffusion and macropore/nanopore models are shown as solid and dashed lines, with confidence intervals shown as thin lines.

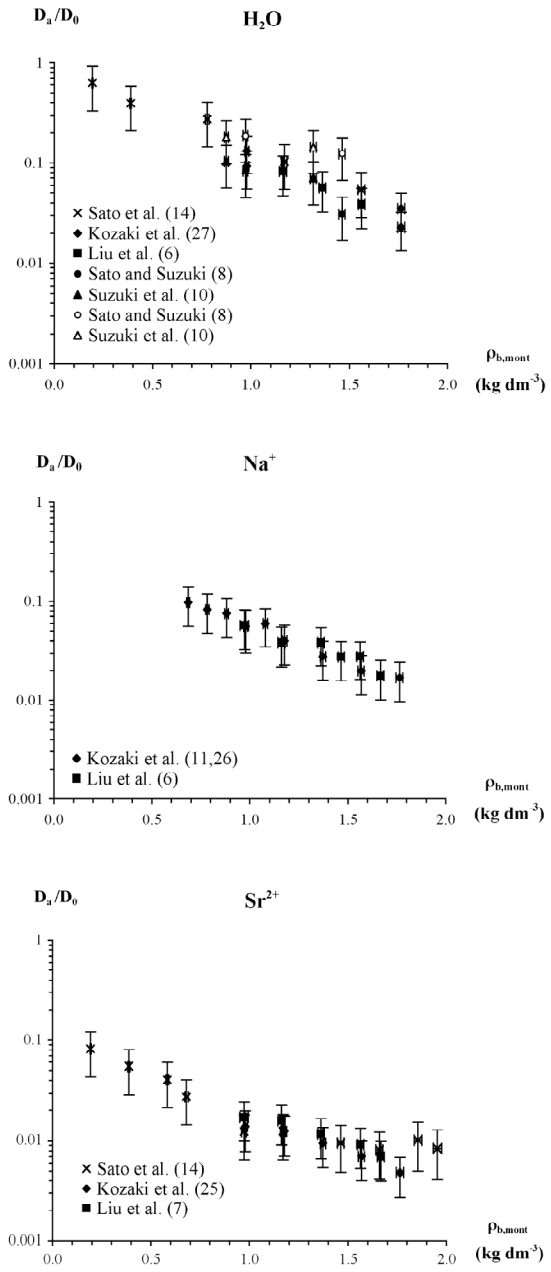
D_a/D_0
H_2O
1
0.1
0.01
0.001
0.0
0.5
1.0
1.5
2.0
$\rho_{b,mont}$
(kg dm^{-3})
× Sato et al. (14)
◆ Kozaki et al. (27)
■ Liu et al. (6)
● Sato and Suzuki (8)
▲ Suzuki et al. (10)
○ Sato and Suzuki (8)
△ Suzuki et al. (10)
D_a/D_0
Na^+
1
0.1
0.01
0.001
0.0
0.5
1.0
1.5
2.0
$\rho_{b,mont}$
(kg dm^{-3})
◆ Kozaki et al. (11,26)
■ Liu et al. (6)
D_a/D_0
Sr^{2+}
1
0.1
0.01
0.001
0.0
0.5
1.0
1.5
2.0
$\rho_{b,mont}$
(kg dm^{-3})
× Sato et al. (14)
◆ Kozaki et al. (25)
■ Liu et al. (7)

Figure 1.

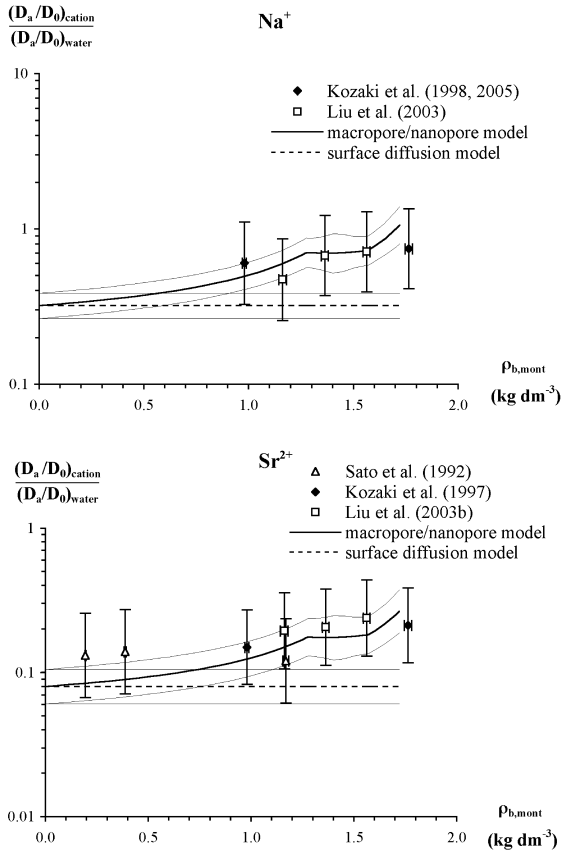
$(D_a/D_0)_{cation}$ / $(D_a/D_0)_{water}$
Na^+
Kozaki et al. (1998, 2005)
Liu et al. (2003)
macropore/nanopore model
surface diffusion model
10
1
0.1
0.0
0.5
1.0
1.5
2.0
$\rho_{b,mont}$
(kg dm^{-3})
$(D_a/D_0)_{cation}$ / $(D_a/D_0)_{water}$
Sr^{2+}
Sato et al. (1992)
Kozaki et al. (1997)
Liu et al. (2003b)
macropore/nanopore model
surface diffusion model
1
0.1
0.01
0.0
0.5
1.0
1.5
2.0
$\rho_{b,mont}$
(kg dm^{-3})

Figure 2.